Natural Hazards (2023) 118:2285–2307
https://doi.org/10.1007/s11069-023-06091-x

ORIGINAL PAPER

The influence of large-scale climate modes on tropical cyclone tracks in the southwest Pacific

Krishneel K. Sharma[1] · **Danielle C. Verdon-Kidd**[1] · **Andrew D. Magee**[1]

Received: 27 November 2022 / Accepted: 29 June 2023 / Published online: 17 July 2023

Abstract

Tropical cyclones (TCs) impact the economy, properties, lives and infrastructure of island nations and territories of the southwest Pacific (SWP), accounting for three in four regional disasters each year. To increase the resilience of the SWP to the destructive impacts of TCs, improved TC track forecasts are needed since a high degree of uncertainty exists around the likely path a TC will take in this region post-formation. This requires better comprehension of the factors contributing to TC track variability occurring at different timescales. Therefore, we examine the modulating impact of key Indo-Pacific climate drivers: the El Niño-Southern Oscillation (ENSO), Interdecadal Pacific Oscillation (IPO), Southern Annular Mode (SAM) and the Indian Ocean Dipole (IOD), on SWP TC track variability. We present new insights into the spatial (*i.e.* prevailing trajectories) and temporal (i.e. track length, average speed and duration) components of TC tracks, being modulated by both individual and combined climate modes. Overall, TC tracks tend to shift northeast during El Niño, IPO positive, IOD east positive and/or SAM negative phases (with a southwest shift observed during the opposite climate phases). Further, we show that when two of these climate modes are in their positive phase (*e.g.* El Niño with the positive phases of IPO or eastern pole of IOD and SAM), TC track length and average speed are enhanced. However, for cases where either one (e.g. El Niño/negative phase of IPO and IOD east) or two (La Niña/negative phase of IPO, IOD east and SAM) climate modes were in the negative phase, an increase in TC track duration was observed. The findings of this study may be used to improve TC forecasting and better quantify TC-related risks.

Keywords ENSO · IPO · SAM · IOD · Multimodal · Southwest Pacific · Tropical cyclone tracks

✉ Krishneel K. Sharma
Krishneel.Sharma@uon.edu.au

[1] School of Environmental and Life Sciences, College of Engineering, Science and Environment, The University of Newcastle, University Drive, Callaghan, NSW 2308, Australia

1 Introduction

Tropical cyclones (TCs) are the most damaging natural hazard (Stephens and Ramsay 2014) that occur across seven basins with a global average of 86 TCs per year (Murakami et al. 2020). Of those, approximately 12–13 TCs occur across the southwest Pacific (SWP; 0°–35°S, 135°E–120°W) (Fig. 1, panel a) region every season (November–April) (Diamond et al. 2013), causing significant impacts on properties, lives and infrastructure. Home to 15 diverse island nations and territories, the population of the SWP are highly vulnerable to the impact of TCs, which have accounted for approximately 1350 deaths since 1950 (EM-DAT 2020). The region's vulnerability to TC impacts (as well as other forms of natural hazards) can be attributed to the geographical location and varying topographies of SWP nations and territories. In addition, most of the population is located no farther than 10 km from the coast (Andrew et al. 2019) for reasons including accessibility to subsistence resources (i.e. dependence upon the ocean for food supply), trade and transport and economic development (Small and Nicholls 2003; Neumann et al. 2015). As such, this means that many vulnerable communities reside in the low-elevation coastal zones, which are highly vulnerable to both short-term (e.g. TCs, storm surges, tsunamis) and long-term (e.g. a rise in sea level) natural disasters (Naylor 2015).

The impact of TCs on the SWP island nations and territories depends on their trajectory (Saverimuttu and Varua 2017), as they often deviate from their modelled/predicted paths and sometimes display erratic behaviour. While most TCs in the SWP region move towards the east/southeast, with few moving towards the west (Holland and Gray 1983), their orientation can be anywhere from the northwest to the southeast (Terry 2007). TCs are also known to meander or oscillate around this mean path (Holland and Lander 1993), with tracks often characterised in terms of duration (long-/short-lived), speed (slow-moving/fast-moving), direction (differing from the expected trend) and shape (from straight to erratic/looping), or a combination of all the above. Erratic behaviour displayed by TC tracks is a distinct feature of the SWP basin compared to other TC basins across the globe (Australian Bureau of Meteorology 2020). As identified by Sharma et al. (2021), TCs take different paths than expected, representing different risks to island nations. Erratic TC tracks are more common within the Coral Sea region; however, the long-term trend also indicates potential changes in the morphology of tracks (as more convoluted contrary to being mostly straight type) within the eastern part of SWP (Sharma et al. 2021). Further, research has highlighted recent variations in TC tracks in the form of poleward shifts, i.e. TCs transition into mid-latitudes or extratropical cyclones (Sinclair 2002; Christensen et al. 2013; Kossin et al. 2014; Sharmila and Walsh 2018). This changing vulnerability for certain island nations to TC track exposure requires further investigation to understand how, where, when and why TCs track across the SWP (post-formation) and impact island nations (either passing by an island nation or making landfall).

The SWP is exceptionally dynamic, and TC activity within the region is modulated by a number of large-scale modes of climate variability operating within and outside of the region (Grant and Walsh 2001; Camargo et al. 2010; Chand et al. 2013; Diamond et al. 2013; Diamond and Renwick 2015; Magee et al. 2017; Magee and Verdon-Kidd 2018). These modes operate over seasonal through to multi-year cycles and include the El Niño-Southern Oscillation (ENSO), Interdecadal Pacific Oscillation (IPO), Indian Ocean Dipole (IOD), Southern Annular Mode (SAM) and Madden Julian Oscillation (MJO). While many previous studies have focused on TC genesis, few studies have

shown the potential impact of these large-scale drivers on TC track morphology, except for the well-known ENSO, where it has been shown that TC tracks follow its well-established influence, that is, east-northeast modulations during El Niño (EN) and west-southwest during La Niña (LN) (e.g. Sinclair 2002; Chand and Walsh 2009; Malsale 2011; Ramsay et al. 2012).

Similar to ENSO but operating on decadal and multidecadal timescales, the IPO is also known to modulate TC activity within the SWP region (Grant and Walsh 2001; Magee et al. 2017). However, studies linking the impact of IPO on SWP TCs are limited—mainly due to the question of the reliability of TC data from the pre-satellite era (before 1970) (Holland 1981). Since IPO is a multidecadal phenomenon, long-term data sets are imperative for analysing relationships. Initial investigations by Grant and Walsh (2001) found that IPO negative conditions resulted in more landfalling TCs across eastern Australia, driven by more favourable wind shear conditions towards the continent; however, their analysis was temporally limited to 1996. Magee et al. (2017) investigated the impact of the IPO on TC genesis and found that IPO positive (negative) conditions result in a northeast (southwest) migration of TC activity, regardless of the ENSO phase. However, to date, no studies have investigated the impact of IPO variability and how the co-occurrence of particular ENSO/IPO phases can influence SWP TC tracks.

Other than Pacific drivers (ENSO and IPO), the other modes of climate variability known to influence SWP (or wider SH) TCs include the SAM and Indian Ocean sea surface temperature (SST) variability (Kidson and Sinclair 1995; Ashok et al. 2007; Renwick and Thompson 2006; Christensen et al. 2013; Saha and Wasimi 2013; Diamond and Renwick 2015; Ramsay et al. 2017; Magee and Verdon-Kidd 2018). Kidson and Sinclair (1995) noted that variation in the SAM resulted in the substantial north–south migration of storm tracks in the Southern Hemisphere (SH). Diamond and Renwick (2015) reported that SAM has no significant impact on SWP TC activities, i.e. TC genesis, tracks and intensity, but influences TC transition into extratropical cyclones near New Zealand.

Indeed, previous studies (e.g. Yin 2005; Kidston and Gerber 2010; Christensen et al. 2013) have emphasised on the projected poleward migration of storm tracks by the high index state of the SAM, augmented by the increased surface temperature gradient, poleward shifts in the wind stress and precipitation. Thus, further work is needed to understand the influence of the SAM on these factors. While the influence of Indian Ocean SST variability on SH TC activity has been widely investigated, there are fewer studies accounting for their influence on SWP TC tracks. Saha and Wasimi (2013) highlighted the link between Indian Ocean SST variability and Australian/SWP TC activity. Magee and Verdon-Kidd (2018) revealed a new relationship between the Indian Ocean SST variability and SWP TC genesis. Anomalously warm (cool) SSTs in the Indian Ocean resulted in a northeasterly (southwesterly) shift in TC genesis, even during ENSO neutral conditions. They also hinted that their findings might have significant implications for TC tracks in the SWP region.

The climate modes discussed here do not operate in isolation, and as such, the prevailing environmental conditions across the SWP represent the combined influence of these individual modes of variability. Magee et al. (2017) have shown that when the suites of climate drivers are considered in co-occurrence, the location of TC genesis is significantly shifted, raising the question of how this may impact the entire TC track. Therefore, this paper aims to investigate the spatio-temporal influence of climate drivers (both individually and coupled) on the SWP TC tracks and their morphology. The following objectives will be addressed to achieve this aim:

Fig. 1 The spatial extent of the southwest Pacific region (0°–35°S, 135°E–120°W) is represented by the blue dashed line with all the TC tracks from 1948 to 2021 shown in grey in panel a. Indicative locations of climate driver indices, including Niño3.4 (ENSO), IOD E (eastern pole of Indian Ocean Dipole) and SAM between 40°S and 65°S. Note: IPO is shown as an oval for illustrative purposes only but is represented by the Tripole Index (TPI), calculated from three oceanic boxes. Exclusive Economic Zones in panel b highlight SWP island nations and atoll nations and territories considered in this analysis. Panels c-f illustrate the timeseries of each climate indices averaged between November and April, depicting positive (red), negative (blue) and neutral (grey) phases. Note that filtered TPI represents IPO until 2015

(1) Investigate the individual influence of Pacific (ENSO and IPO) and remote climate drivers (Indian Ocean SST variability and SAM) on SWP TC track activity.
(2) Explore the combined influence of Pacific and remote drivers on the spatio-temporal variability of SWP TC tracks.
(3) Assess how climate mode modulation of TC tracks alters the likelihood of TCs passing over or by each island nation in the SWP.

Identifying how climate drivers interact at varying timescales (interannual and interdecadal), and contribute to spatio-temporal variability of SWP TC tracks, may enable meteorologists and forecasting agencies to produce more reliable TC forecasts and seasonal outlooks and allow better decision-making when planning for future TC events. The findings could complement existing TC outlooks with more information on probable track trajectories to increase societies' resilience to the destructive impacts of TCs by estimating the location of landfall/impact once a TC forms.

2 Data and methods

2.1 TC track data

This study uses the South Pacific Enhanced Archive of Tropical Cyclones (SPEArTC) database for best track TC data, spanning between 1948 and 2021, with track locations available at 6-h intervals for the entire TC lifecycle (Diamond et al. 2012). The first point of each unique track in the SPEArTC data set is considered as the TC genesis point (TC formation), and the last point as the TC decay point (i.e. where TC ended/terminated). This data set was chosen because it is considered the most complete repository of TC data for the SWP region (Magee et al. 2016; Sharma et al. 2020).

2.2 Climate indices

The climate modes investigated in this study include ENSO, Indian Ocean SST variability, IPO and SAM—a diagrammatic summary is illustrated in Fig. 1 (panel a) along with their timeseries (panels c-f). Further details on how each index was derived are described below:

- ENSO index: monthly Oceanic Niño Index (ONI) utilised in this study was obtained from the National Oceanic and Atmospheric Administration (NOAA), Climate Prediction Centre (Kousky and Higgins 2007). ONI is based on the 3-month running mean of Extended Reconstructed Sea Surface Temperature Version 5 (ERSSTv5) (Huang et al. 2017a; 2017b) sea surface temperature (SST) anomalies in the Niño3.4 region

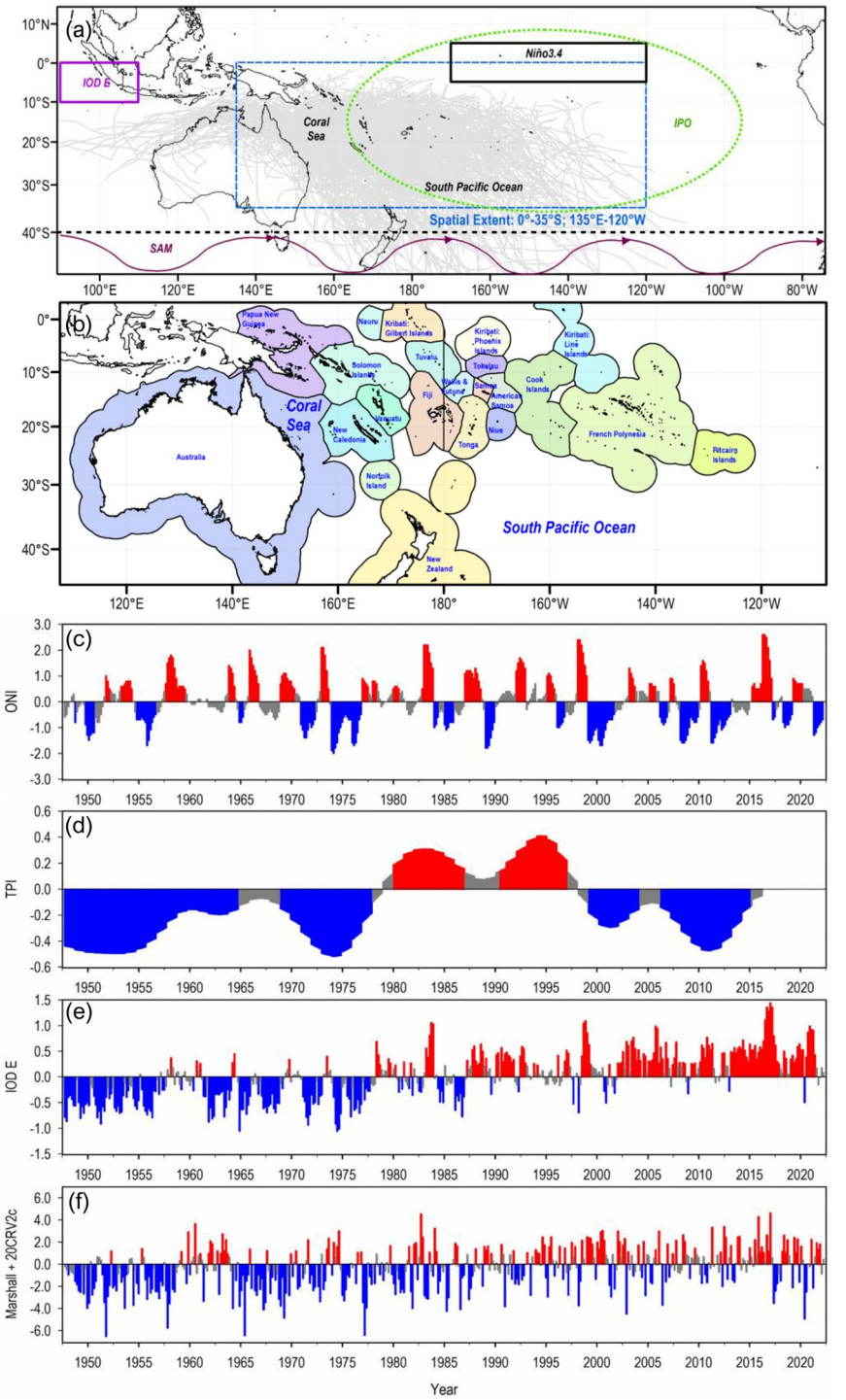
(a)
Niño3.4
IOD B
Coral Sea
IPO
South Pacific Ocean
Spatial Extent: 0°-35°S; 135°E-120°W
SAM
(b)
Coral Sea
South Pacific Ocean
Australia
(c)
ONI
(d)
TPI
(e)
IOD E
(f)
Marshall + 20CRV2c
Year

(5°N–5°S, 120°–170°W). The anomaly calculation of ONI is based on the multiple-centred 30-year base period, which is updated every five years. This approach ensures that the classification of EN and LN events is defined by their contemporary climatology and remains fixed over most of the historical period. A threshold of ± 0.5 °C is used to define the EN and LN phases when the periods of below-/above-average SSTs occur for at least five consecutive overlapping seasons, while SSTs in-between are classified as ENSO neutral events.

- IPO Index (Tripole Index [TPI]): calculated as the difference between the average SST anomalies over the central equatorial Pacific (10°S–10°N, 170°E–90°W) and the average of the SST anomalies in the Northwest Pacific (25°N–45°N, 140°E–145°W) and Southwest Pacific (50°S–15°S, 150°E– 60°W). The TPI is calculated using ERSSTv5 SST anomalies derived from NOAA and is available in filtered and unfiltered versions. For the present study, the filtered IPO was used that is obtained by applying a 13-year Chebyshev low-pass filter (Henley et al. 2015), covering the period from 1948 to 2015.
- IOD E (eastern Indian Ocean dipole): monthly SST anomalies within the south-eastern Indian Ocean (0°–10°S, 90°E–110°E), whereby positive (negative) IOD E phase indicates warmer (cooler) SSTs (Saji et al. 1999). We also investigated the Dipole Mode Index; however, we found that the eastern pole of the Indian Ocean Dipole has the greatest impact, which is consistent with studies on TC genesis (Magee and Verdon-Kidd 2018).
- SAM: is the monthly differences in the mean sea level pressure observed from six *in-situ* stations close to 40°S and 65°S (Marshall 2003; Ho et al. 2012; Diamond and Renwick 2015) and is calculated using the following equation after Gong and Wang (1999):

$$\mathrm{SAM} = \mathrm{P}^{*}_{40^{\circ}\mathrm{S}} - \mathrm{P}^{*}_{65^{\circ}\mathrm{S}} \tag{1}$$

Based on the recommendations of Ho et al. (2012) and its application on SWP TCs (Diamond and Renwick 2015), the Marshall Index was selected, which is available since 1957. To extend the SAM index to match the start date of the present study (1948), 20th Century Reanalysis Version 2c (20CRv2c) sea level pressure data, available from 1851 to 2011, were used (Gong and Wang 1999). Prior to merging, the zonal mean of the Marshall Index was standardised using a similar climatological baseline as 20CRv2c (1981–2010). SAM was then calculated using Eq. 1.

The monthly anomaly values for all climate indices were calculated using the 1981–2010 climatological baseline, except for TPI (which uses the 1971–2000 baseline) (World Meteorological Organisation 2017). Each climate mode's positive, negative and neutral phases were defined using a threshold of ± 0.5 standard deviations from the mean.

2.3 Spatio-temporal analysis techniques

The modulation of TC tracks by the climate drivers was assessed in two ways. Firstly, the individual influence of climate drivers on TC tracks was examined spatially through density plots. TC tracks (vector data) were superimposed over 3 × 3° grid cells to transform into a raster. The raster data were normalised according to the length of each climate driver's phase months (seasonal) over 74 years (i.e. from 1948–2021). The difference in TC

track density was then computed between the positive–negative, positive–neutral and negative–neutral phases of each climate driver.

The combined influence of climate drivers on SWP TC tracks was examined by pairing ENSO phases with the positive, negative and neutral phases of other climate modes (IPO and SAM) and indices (IOD E). For example, EN was paired with the positive, negative and neutral phases of IOD E, and TC track trajectories were stratified and analysed for each of these pairings, respectively. A total of 27 pairings were considered in this paper when analysing spatio-temporal modulations in TC trajectories. The temporal characteristics of TC tracks, including duration, track length and average moving speed, were also evaluated for individual climate drivers and the multimode pairings. TC speed in this study is defined as the average moving speed of a TC track over its lifetime and was calculated using the TC track length (km) over its entire duration (in hours), with the assumption that almost all timestamps in SPEArTC are 6-hourly. An unpaired two-tail Student's *t*-test was performed to determine whether the observed differences in TC characteristics between the phases of each climate driver were statistically significant.

Finally, to identify and evaluate how landfall changes during each climate driver's phases (individually and combined) on individual SWP island and atoll nations and territories, we calculated the mean number of TCs per season observed within each island nation's Exclusive Economic Zone, EEZ (Fig. 1, panel b) (Flanders Marine Institute 2018). The EEZ is an area beyond and adjacent to the territorial sea with an outer limit not exceeding 200 nautical miles (Flanders Marine Institute 2018). Note: based on the study region (Fig. 1, panel a), the entire Australian region EEZ is not considered for analysis, but the region straddling the 135°E boundary.

3 Results

3.1 Pacific climate mode influences on TC tracks (ENSO and IPO)

The differenced density plots of SWP TC tracks for EN, LN and ENSO neutral phases are illustrated in Fig. 2 (panels a-c), with the accompanying boxplots showing TC duration, track length and average moving speed (hereafter referred to as average speed) laterally organised in panels d-f. The results of the Student's *t*-test (*p*-values) for all Pacific climate modes are shown in Table 1.

Figure 2 (panels a-c) displays the typical east-northeast and west-southwest modulation of SWP TC activity during EN and LN conditions. New insights are also presented regarding the impact of ENSO on the temporal characteristics of SWP TC tracks (panels d-f). For instance, the duration plots (panel d) reveal that during EN, TC tracks have a shorter lifetime (mean duration of 9.69 days) compared to LN (mean duration of 10.32 days). Conversely, the TC tracks during LN (mean of 3392 km) exhibit longer trajectories than during EN (mean of 3160 km in panel e). Consequently, these attributes result in TCs that are faster-moving (slower-moving) during LN (EN), with a mean speed of 15.32 km/hr (14.27 km/hr). Table 1 and panel f also reveal that TC tracks during LN conditions are significantly faster-moving (compared to neutral conditions).

The implications of TC tracking within each SWP island nation's EEZ during different ENSO phases are shown through the heatmap in panel g. Consistent with the typical east-northeast modulation of TCs by ENSO, several eastern (and some central) SWP nations

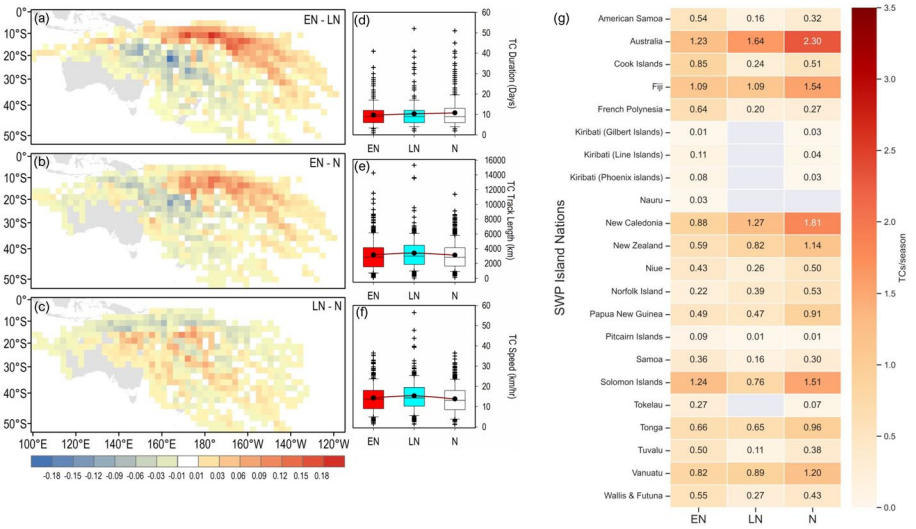

Fig. 2 Difference in SWP TC track (from 1948–2021) density (resolution is 3×3°) between ENSO pairings [El Niño–La Niña (a), El Niño–Neutral (b) and La Niña–Neutral (c)]. Panels d–f show boxplots of TC duration, TC track length and average moving speed according to ENSO phases, respectively. The boxes show the 25th and 75th percentiles, the lines inside the box mark the median, the dots and red line mark the mean, and the crosses mark the outliers (lower 5th and upper 95th percentiles). The heatmap (panel g) demonstrates the TCs/season (Nov-Apr) summary that passed within each EEZ according to each ENSO phase. Grey boxes within the heatmap indicate no TCs/season. El Niño (EN), La Niña (LN), ENSO neutral (N)

Table 1 Student's *t*-test *p*-values comparing the differences between the boxplots of different ENSO and IPO phases for each TC attribute.

TC attributes	Pairings	ENSO	IPO
TC duration	EN/Pos v LN/Neg	0.28	**0.00**
	EN/Pos v N	**0.04**	0.18
	LN/Neg v N	0.45	0.13
TC track length	EN/Pos v LN/Neg	0.23	**0.00**
	EN/Pos v N	0.79	0.22
	LN/Neg v N	0.11	0.13
TC speed	EN/Pos v LN/Neg	0.12	**0.00**
	EN/Pos v N	0.38	**0.00**
	LN/Neg v N	**0.02**	**0.00**

El Niño (EN), La Niña (LN), neutral (N), Positive (Pos) and Negative (Neg)

Bold values denote statistically significant results at the 95% level.

are largely impacted by EN influenced TCs. This includes American Samoa (0.54 TCs/season), Cook Islands (0.85 TCs/season), French Polynesia (0.64 TCs/season), Niue (0.43 TCs/season), Tokelau (0.27 TCs/season), Tonga (0.66 TCs/season), Tuvalu (0.50 TCs/season), Samoa (0.36 TCs/season) and Wallis and Futuna (0.55 TCs/season).

The west-southwest modulation of TCs during LN exhibits TC risk for nations including eastern Australia (1.64 TCs/season), New Caledonia (1.27 TCs/season), New Zealand (0.82 TCs/season), Norfolk Island (0.39 TCs/season) and Vanuatu (0.89 TCs/

season)—nations that are located west of the dateline. Despite their location, southern Papua New Guinea (PNG; 0.49 TCs/season) and Solomon Islands (1.24 TCs/season), both located on the western side of SWP, are also more at risk during EN than LN. At the same time, Fiji is impacted equally by EN and LN TCs (1.09 TCs/season), likely due to its central location within the SWP region. Interestingly, the majority of the island nations are observed to be at more risk during the ENSO neutral phase. This raises the question of whether other climate drivers/indices, present within or outside the SWP region, influence SWP TCs during ENSO neutral.

The spatio-temporal variability during IPO (Fig. 3) indicates increased TC track activity in the central and eastern Pacific during IPO positive (compared to IPO negative), evident in panels a and b of Fig. 3. This differs from the northeast/southwest shift in trajectory observed during ENSO events (Fig. 2). Further, panels d-f and Table 1 confirm that IPO positive (negative) tracks tend to be significantly fast-moving (slow-moving) with an average speed of 15.85 km/hr (13.40 km/hr), but with a shorter (longer) mean lifetime of 9.38 days (10.87 days) and lengthier (shorter) tracks of 3457 km (2951 km) on average.

Indeed, such spatio-temporal modulations also increase the likelihood of risk impact over the SWP island nations, depicted in panel g of Fig. 3. It is observed that during IPO negative periods, higher number of TCs are observed, regardless of the nation's geographical location and/or spatial modulation during the negative phase. The nations with the highest risk during IPO negative phase are located in the western SWP, including Australia (3.16 TCs/season), New Caledonia (2.54 TCs/season), Norfolk Island (0.71 TCs/season), PNG (0.99 TCs/season), Solomon Islands (1.78 TCs/season) and Vanuatu (1.66 TCs/season). Interestingly, the TC risk imposed during IPO negative extends to island nations located east of the dateline—e.g. American Samoa, Cook Islands, Fiji, French Polynesia, Niue, Samoa, Tokelau, Tonga and Wallis and Futuna. Of all three phases, IPO neutral represents the lowest risk of TCs impacting individual EEZs.

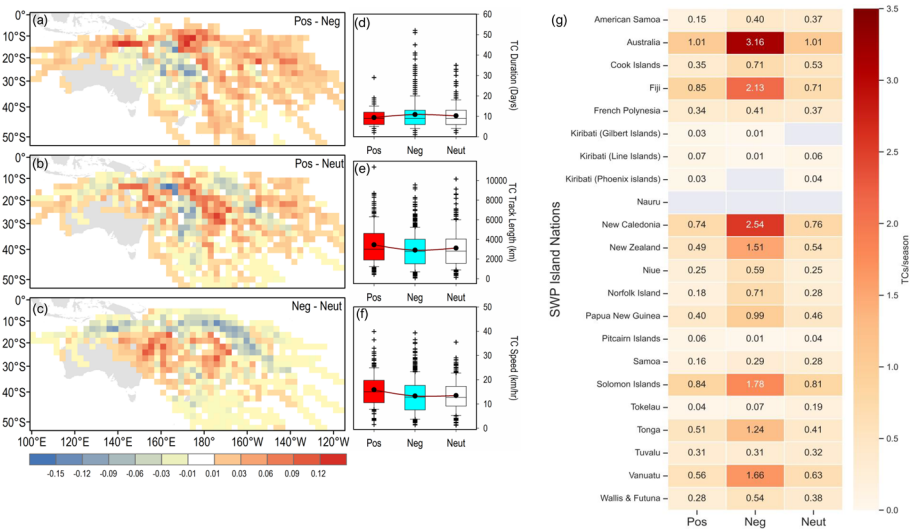

Fig. 3 As in Fig. 2, but for IPO from 1948–2015. IPO positive (Pos), IPO negative (Neg) and IPO neutral (Neut)

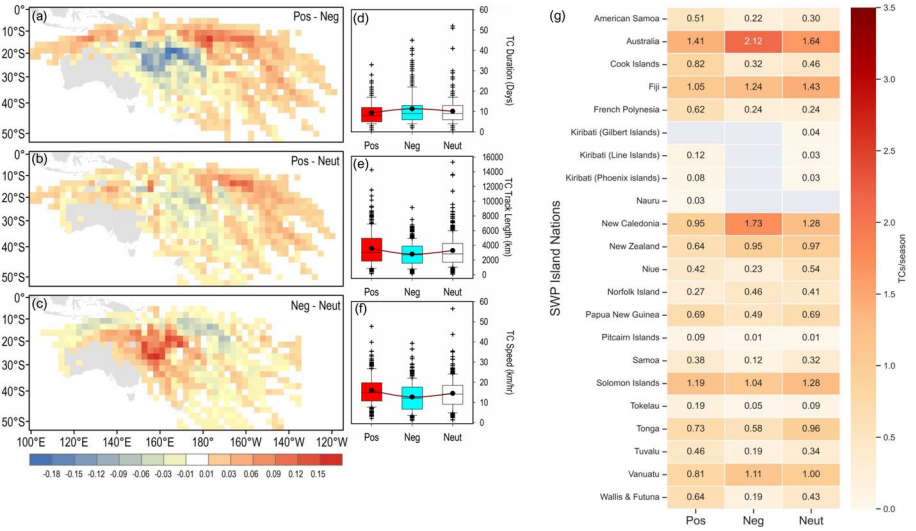

Fig. 4 As in Fig. 2, but for IOD E. IOD E positive (Pos), IOD E negative (Neg) and IOD E neutral (Neut)

Table 2 As in Table 1, but for IOD E and SAM

TC attributes	Pairings	IOD E	SAM
TC duration	Pos v Neg	**0.00**	0.10
	Pos v N	0.11	0.77
	Neg v N	**0.05**	0.14
TC track length	Pos v Neg	**0.00**	**0.00**
	Pos v N	0.13	0.09
	Neg v N	**0.00**	**0.02**
TC speed	Pos v Neg	**0.00**	**0.00**
	Pos v N	**0.01**	**0.03**
	Neg v N	**0.00**	0.06

Bold values denote statistically significant results at the 95% level
Positive (Pos), negative (Neg) and neutral (N)

3.2 Other climate mode influences on TC tracks (IOD E and SAM)

The difference density plots of SWP TC tracks categorised as per IOD E phases are illustrated in Fig. 4 (panels a-c). A clear eastward propagation of TC tracks is observed when SSTs in the northeast Indian Ocean are warmer than average (IOD E positive), while TC tracks are more confined to the west of the study region when IOD E is negative (cool) (panels a-c). In particular, IOD E negative results in a clear elevation of TC tracks frequency around the northeastern coast of the Australia/Coral Sea region (panels a and c)—increasing TC-related hazard (2.12 TCs/season) demonstrated by the density plot in panel g. As evident in the boxplots (panel e) and Table 2, TC tracks associated with IOD E positive are significantly lengthier (3563 km) when compared with IOD E negative (2797 km). These longer trajectories have shorter durations (mean duration of 9.38 days) compared to smaller tracks of TCs that occur during the IOD E negative phase (mean duration of

11.36 days in panel d), and the difference is statistically significant (Table 2). As such, TCs that occur during IOD E positive are significantly faster-moving (15.96 km/hr) compared to TCs occurring in IOD E negative (12.72 km/hr) (panel f). These modulated TCs (during IOD E positive) distinctly increases the risk impact for the majority of the eastern SWP island nations (panel g)—including American Samoa (0.51 TCs/season), Niue (0.42 TCs/season), Pitcairn Islands (0.09 TCs/season), Samoa (0.38 TCs/season), Tokelau (0.19 TCs/season), Tonga (0.73 TCs/season), Tuvalu (0.46 TCs/season) and Wallis and Futuna (0.64 TCs/season).

The risk impact on island nations located from central-to-western SWP is shown to vary. While the typical western SWP island nations such as New Caledonia (1.73 TCs/season), Norfolk Island (0.46 TCs/season) and Vanuatu (1.11 TCs/season) are at risk during IOD E negative, nations such as PNG (0.69 TCs/season) and Solomon Islands (1.19 TCs/season) are vulnerable to IOD E positive influenced TCs. Central SWP island nations such as Fiji & New Zealand (1.24 & 0.95 TCs/season) and Tuvalu (0.46 TCs/season) are at risk during negative and positive IOD E, respectively.

For TCs that occur during negative SAM phases, tracks are shown to migrate further east/northeast when compared to the positive phase, as shown in Fig. 5 (panels a and c). Additionally, the typical influence of SAM positive is evident in panel a, whereby most of the tracks are modulated poleward (i.e. longer tracks of an average of 3585 km; panel e), significantly in contrast to SAM negative (Table 2), which has shorter tracks (average of 2907 km; panel e). In particular, panels a and b demonstrate the influence of SAM positive on the extension of TCs south of ~ 40°S, while during SAM negative, this tends to occur north of ~ 40°S (panel c). Specifically, these longer tracks are characteristic of mid-latitude cyclones (or extratropical cyclones), also reported in Sharma et al. (2021), that tend to continue beyond the tropical latitudes, with fast-moving characteristics during SAM positive. This is important as the extension of TC tracks beyond tropical latitudes (transition into mid-latitudes) tends to impact New Zealand (0.66 TCs/season, panel g). During SAM positive, the extension of TC tracks is coupled with increased speed (mean speed of 15.80 km/

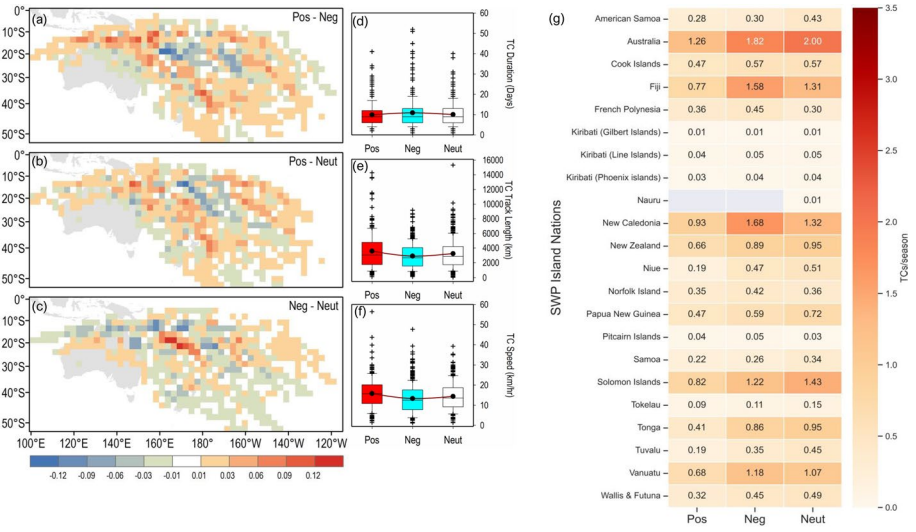

Fig. 5 As in Fig. 2, but for SAM. SAM positive (Pos), SAM negative (Neg) and SAM neutral (Neut)

hr) and a mean lifetime of 9.89 days. Severe TC Gita (2018) is one such example, where SAM was in a neutral-to-weak positive phase (Australian Bureau of Meteorology 2018), that transitioned into an extratropical cyclone impacting New Zealand. Conversely, TC tracks influenced by SAM negative tend to be slower-moving (mean speed of 13.33 km/hr) but with an extended duration (mean of 10.88 days).

Almost all SWP island nations are susceptible to a higher number of TCs within their EEZ when the SAM is positive, except for New Zealand, which is a result of the poleward shift during negative SAM. Panel g demonstrates that New Zealand is more vulnerable during SAM negative (0.89 TCs/season) and SAM neutral (0.95 TCs/season).

3.3 Multimodal modulation of SWP TC tracks

The preceding section demonstrated that both Pacific and remote large-scale climate modes modulate TC track variability in terms of position, duration, speed and length. However, none of these modes operates in isolation and may act to enhance or suppress the impact of each other. As such, the following sections explore the coupled influence of IPO, IOD E and SAM with the canonical ENSO on TC tracks in the SWP.

3.3.1 Co-influence of ENSO and IPO on TC tracks

To evaluate the co-influence of ENSO and IPO phases on SWP TC track variation, each phase of ENSO (i.e. EN, LN and ENSO neutral) was paired with the positive, negative and neutral phase of IPO, as shown in Fig. 6 (panels a-c). The temporal characteristics, such as the duration (panels d-f), average speed (panels g-i) and track lengths (panel j-l) and their statistical difference (shown as *p*-values) in the last row, were also analysed.

Figure 6 highlights a higher proportion of TCs in IPO negative for all ENSO phases in panels a-c. Panel b illustrates how TC tracks shift westward during LN/IPO negative, whereas the pairing of EN/IPO positive distinctly shows enhanced eastward modulation (east of 150°W) of TC tracks (panel a), consistent with observed relationships with TC genesis by Magee et al. (2017). The EN/IPO positive pairing is particularly important for nations towards the eastern SWP, including French Polynesia, the Pitcairn Islands and the Line Islands of Kiribati, where TCs are relatively infrequent compared to the western SWP (Magee et al. 2020; Sharma et al. 2021). Indeed, the heatmap depicting the average number of TCs per season for this multimodal pairing further enhances our understanding of the potential risk of impact to each SWP island nation, atolls and territories (Fig. 7). For instance, the above-mentioned island nations are shown to be impacted mostly during EN/IPO positive than other phase pairings—e.g. French Polynesia (0.19 TCs/season). This is consistent and further complements the increased risk impact demonstrated individually by EN (Fig. 2) and IPO positive (Fig. 3).

Figure 6 further demonstrates modulation in the TC track attributes, which either has been enhanced or suppressed when compared to the typical influence of ENSO only in Fig. 2. For example, the interaction between IPO positive and EN tracks exhibits an average track length of 3577 km and average speed of 16.26 km/hr (panels d and g)—a substantial increase of 13% and 14% when compared to EN TCs in Fig. 2. A negligible difference in duration was observed between IPO positive and EN tracks (suppressed by 3%) (panel j). Conversely, the combined influence of LN/IPO negative influenced the mean duration of 10.76 days (a 4% enhancement) while suppressing track length (3336 km) and average speed (14.90 km/hr) by 2 and 3%, respectively, when compared to the individual

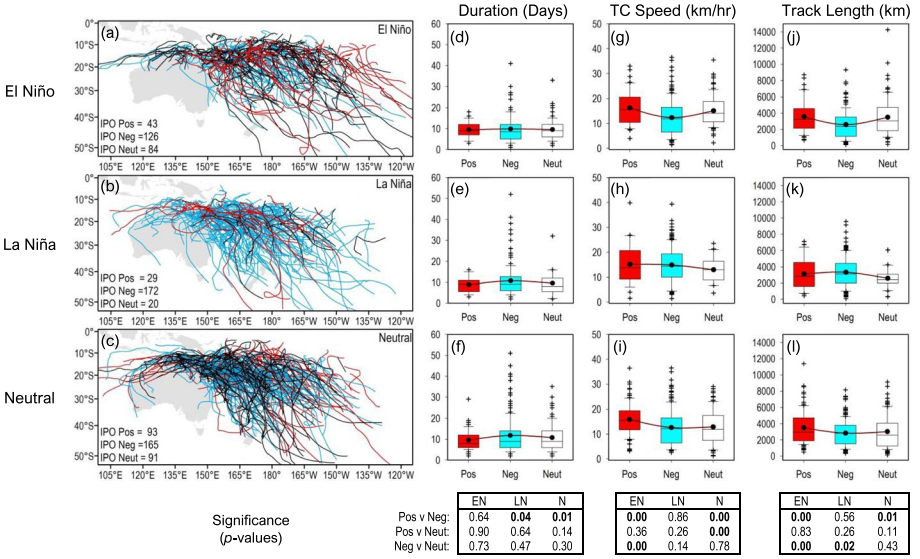

Fig. 6 TC tracks categorised as per pairing of ENSO and IPO phases from 1948–2015. Left panels: El Niño **a**, La Niña **b** and ENSO neutral **c** TC tracks coupled with IPO positive (red), negative (blue) and neutral (black) phases. The number of TC tracks for each climate mode pairing is shown on the bottom-left of each panel. The boxplots demonstrate the TC duration (**d–f**), average moving speed (**g–i**) and TC track length (**j–l**) related to the coupling of ENSO and IPO phases (row-wise). The boxes show the 25th and 75th percentiles, the lines inside the box mark the median, dots and red line mark the mean, and crosses mark the outliers (lower 5th and upper 95th percentiles). The bold values (*p*-values) in the last row denote that differences between the boxplots of multimodal pairings (for each TC attribute) are statistically significant at the 95% level, as per Student's *t*-test

influence of LN on TC tracks in Fig. 2 (panels d-f). Furthermore, the dominant influence of IPO negative is exhibited through the westward modulation of EN tracks in panel a, with a reduction in length (18%) and average speed (13%), and the difference is statistically significant (Fig. 6).

The dominant influence of IPO negative over ENSO impacts on TC tracks is also illustrated through the heatmap (Fig. 7). It is shown that most SWP island nations, atolls and territories are impacted when IPO negative is coupled with all three ENSO phases, i.e. EN, LN or ENSO neutral. Importantly, eastern Australia's highest risk occurs during the LN/IPO negative combination (1.34 TCs/season in Fig. 7, central column), given TC tracks are modulated further west (Fig. 6, panel b). Additionally, Fig. 7 potentially provides additional insight into the cause of the observed elevated risk over PNG and Solomon Islands (western SWP nations, Fig. 2, panel g) that appeared to be unusual based on the location of these islands.

3.3.2 Co-influence of ENSO and IOD E on TC tracks

Complimentary to their individual influences (in Figs. 2 and 4), the combination of positive (negative) phases of ENSO and IOD E also results in east-northeast (west-southwest) modulation of TC tracks (Fig. 8, panels a and b). EN is more likely to co-occur with IOD E positive (159 TCs) and LN tends to occur with IODE negative (108 TCs), consistent

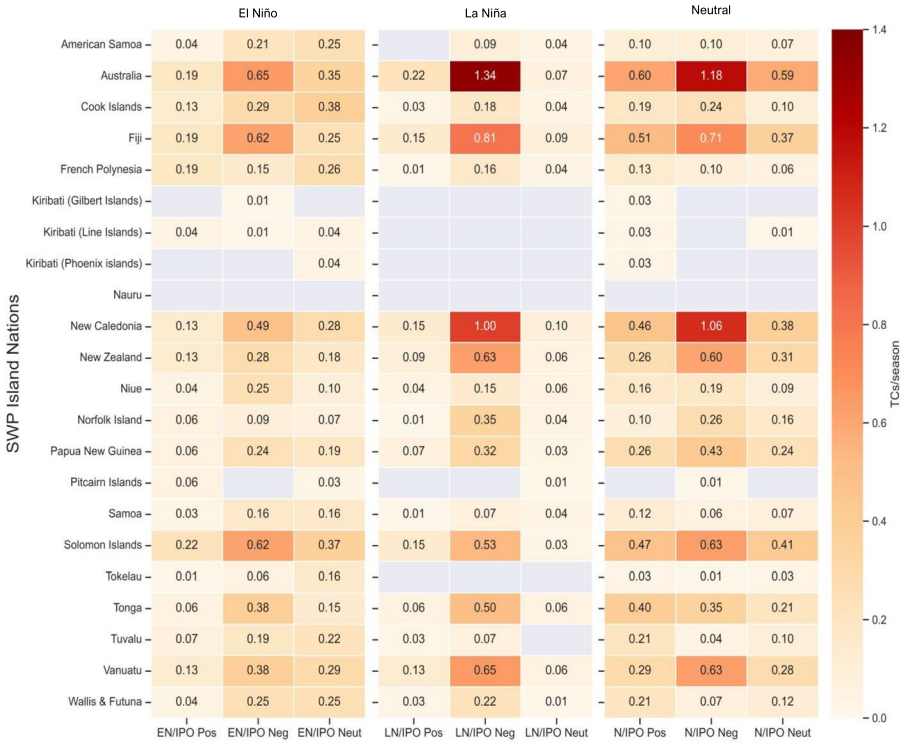

Fig. 7 The heatmap demonstrates the summary of TCs/season (Nov-Apr) that passed within each EEZ during ENSO phases when coupled with IPO phases between 1948–2015. The left column exhibits risk impact for El Niño, the central column for La Niña and the right column for ENSO neutral, coupled with IPO positive (Pos), negative (Neg) and neutral (Neut) phases. Grey boxes within the heatmap indicate no TCs/season

with Liu and Chan (2012) and Magee and Verdon-Kidd (2018). Furthermore, positive phases of IOD E contribute significantly to increased TC track lengths during EN phases, while the converse occurs for IOD E negative LN combinations. Compared to ENSO alone (Fig. 2), which generally results in LN associated tracks being slightly faster-moving than EN (15.32 vs 14.27 km/hr), the co-influence of IOD E positive phase results in TCs during EN being faster-moving (average speed of 15.53 km/hr; Fig. 8, top row) than during LN/IOD E negative (average speed of 14.41 km/hr; Fig. 8, panel h). The heatmap generated for ENSO and IOD E combinations in Fig. 9 illustrates the risk of TCs impacting SWP island nations is substantially different for EN/IOD E positive and LN/IOD E negative. EN/IOD E positive tends to impact almost all SWP island nations in contrast to the other two IOD E phases with EN (left column). The LN/IOD E pairings (central column) is shown to mainly impact eastern Australia (0.84 TCs/season), Fiji (0.43 TCs/season), New Caledonia (0.61 TCs/season), New Zealand (0.36 TCs/season), Vanuatu (0.35 TCs/season) and Solomon Islands (0.30 TCs/season)—whereby majority of these nations are on the western part of SWP (or west of the dateline).

Interestingly, under ENSO neutral/IOD E negative conditions, there is an observed increase in TC occurrence (163 TCs) in panel c (Fig. 8), indicating that IOD E negative can influence SWP TCs independent of ENSO influence (since ENSO is neutral in these cases).

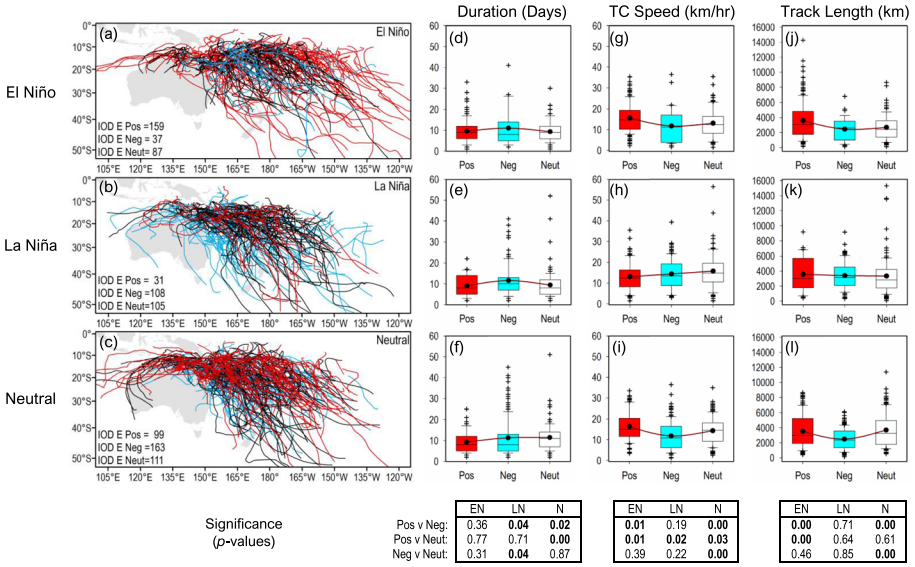

Fig. 8 As in Fig. 6 but for the pairing of ENSO and IOD E phases from 1948–2021

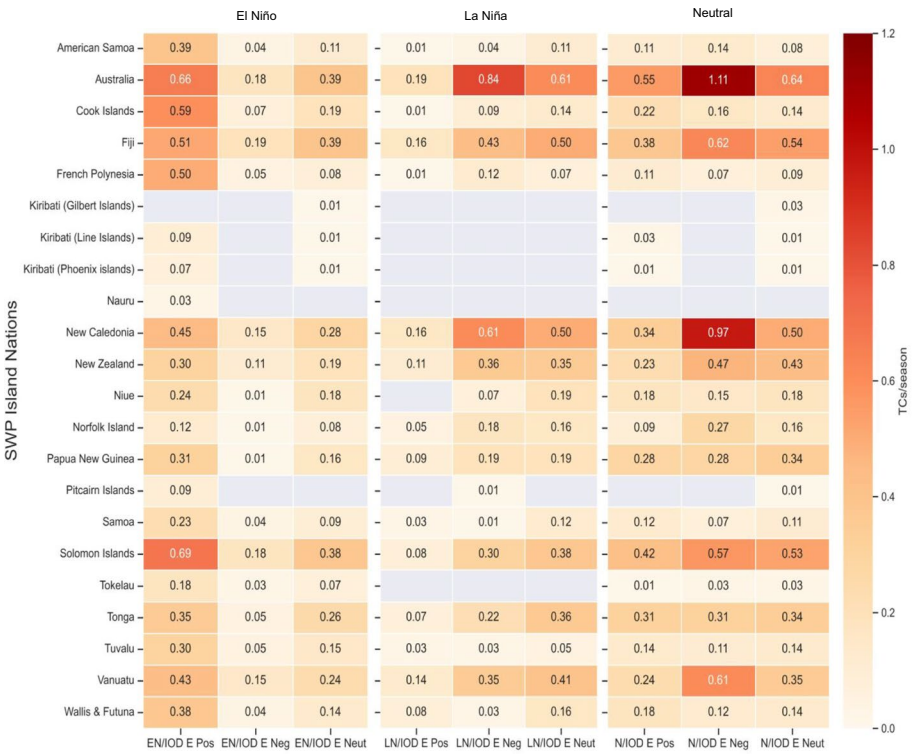

Fig. 9 As in Fig. 7 but for ENSO and IOD E phases from 1948–2021

A similar finding was reported by Magee and Verdon-Kidd (2018), where it was shown that regardless of ENSO (i.e. during ENSO neutral conditions), Indian Ocean SST variability also spatially modulates SWP TC genesis. Nevertheless, compared to ENSO neutral, TC tracks during ENSO neutral/IOD E negative display a reduction in length (2480 km compared to 3392 km) with an extended lifetime (11.28 days compared to 10.32 days), indicative of a slow-moving nature (average speed of 11.82 km/hr compared to 15.32 km/hr) (Fig. 8, panels f, i and j) when compared with the track attributes during ENSO neutral in Fig. 2. TCs of this nature tend to be impactful for island nations similar to those mentioned above for LN/IOD E, but with an enhanced number of TCs per season (Fig. 9, right column)—e.g. Australia (1.11 TCs/season), New Caledonia (0.97 TCs/season), Fiji (0.62 TCs/season), Vanuatu (0.61 TCs/season), Solomon Islands (0.57 TCs/season) and New Zealand (0.47 TCs/season).

3.3.3 Co-influence of ENSO and SAM on TC tracks

The SAM modulates the impact of ENSO on TC tracks by suppressing or magnifying the typical ENSO track characteristics (Fig. 10). Spatially, the TC tracks during SAM negative (in all three ENSO phases) are extended further east than SAM positive tracks that are more confined westward (panels a-c). Temporally, the negative and neutral phases of SAM result in enhanced TC occurrences during EN (112 and 101 TCs), LN (91 and 88 TCs) and ENSO neutral (136 and 141 TCs) as compared to SAM positive (which suppresses ENSO-based TC frequency). Indeed, enhanced TC frequency indicates greater risk impacts for SWP island nations, atolls and territories. Figure 11 demonstrates (through larger TCs/season values) that many island nations tend to get impacted mostly when SAM negative is associated with all three phases of ENSO. Most of these include eastern Australia, Fiji, New Caledonia, Solomon Islands, Vanuatu, New Zealand and Tonga, with average TCs ranging from 0.27 to 0.78 per season.

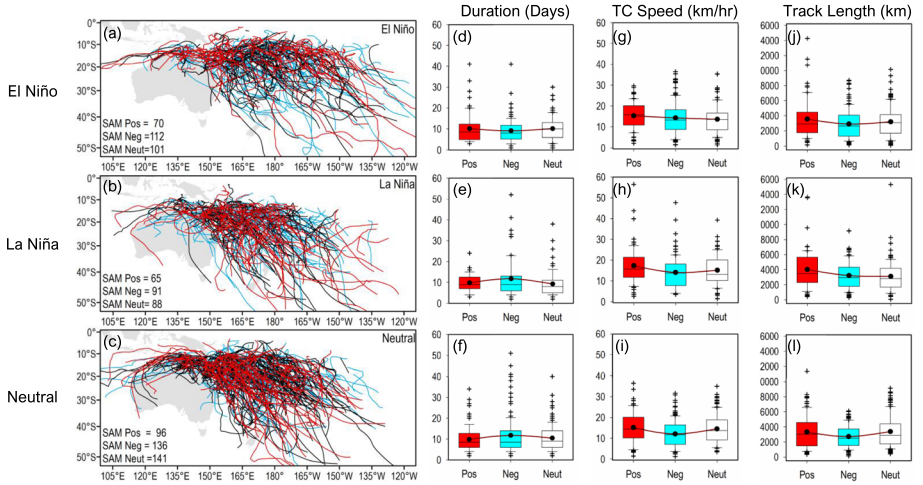

Fig. 10 As in Fig. 6 but for the pairing of ENSO and SAM phases from 1948–2021

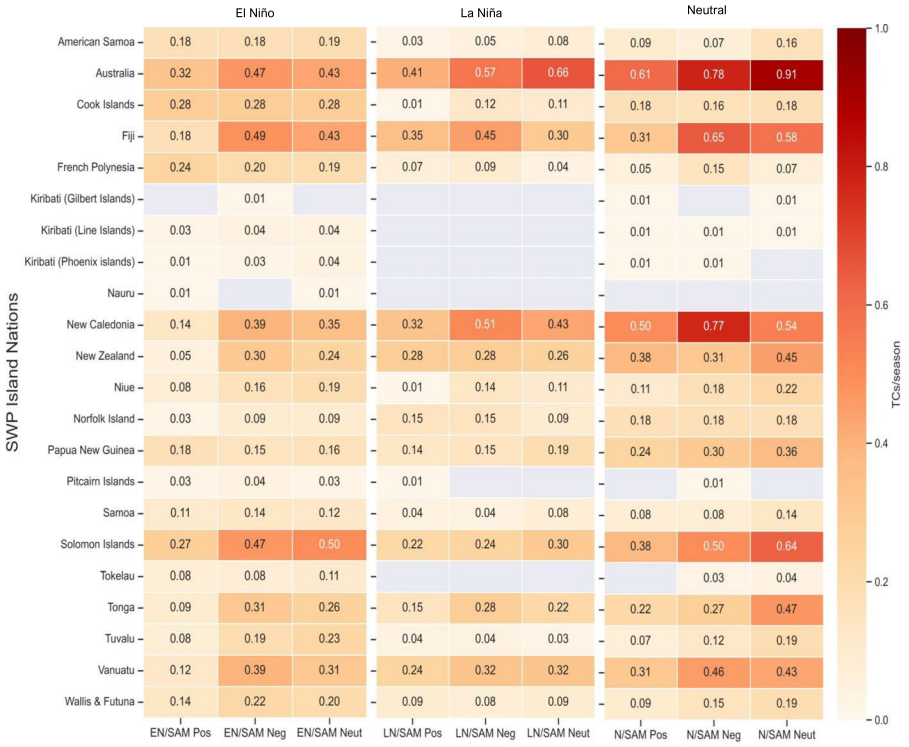

Fig. 11 As in Fig. 7 but for ENSO and SAM phases from 1948–2021

The *p*-values in the last row (of Fig. 10) demonstrate significant temporal modulations mostly during LN and SAM positive phase pairings—with TCs being lengthier (4024 km) yet faster-moving (17.32 km/hr). Indeed, this is somewhat similar to the individual influence of ENSO and SAM portrayed in Figs. 2 and 5, respectively, where LN TCs were found to be fast-moving, and tracks were also lengthier during SAM positive. Additionally, TCs during LN/SAM positive are shown to typically impact island nations central-to-western SWP—eastern Australia (0.41 TCs/season), New Caledonia (0.32 TCs/season) and Fiji (0.35 TCs/season) and, to some extent, New Zealand (0.28 TCs/season) and Vanuatu (0.24 TCs/season), as shown in Fig. 11 (central column).

4 Discussion

This paper aimed to evaluate the spatio-temporal influence of climate drivers on SWP TC track activity. To achieve this, Pacific (ENSO and IPO) and remote (IOD E and SAM) drivers of climate variability were investigated in terms of their spatio-temporal influence on TC tracks and related attributes, both individually and in co-occurrence. Additionally, the hazard presented by the number of TCs intercepting the EEZ boundary for each island nation was evaluated in response to the modulation of TCs by the ocean–atmospheric interactions, both individually and coupled.

4.1 Variability in TC tracks by individual climate drivers

Both Pacific climate drivers (ENSO and IPO) exhibited eastern and western modulation of SWP TC tracks during positive and negative phases, respectively—consistent with previous studies (e.g. Grant and Walsh 2001, Chand and Walsh 2009; Camargo et al. 2010; Chand et al. 2013; Magee et al. 2017). Building upon previous research that were mostly on TC genesis, our findings illuminate additional impacts on track characteristics. It is revealed that TC tracks associated with EN (LN) are slow-moving (fast-moving) with reduced (extended) TC lifetime (Fig. 2, panels d and f)—with the latter attribute (i.e. shorter lifetime) being consistent with Ramsay et al. (2012). EN influenced TCs being slow-moving is in contrast with Sinclair's (2002) findings, which generally suggested otherwise; however, this could be due to the longer dataset used in this study and differences in the approach for calculating TC speed between the studies.

Similar to Magee et al. (2017), who reported clustering of TC genesis points around central SWP during IPO positive, our findings also demonstrate comparable variability for TC tracks, i.e. increased TC activity around this region (Fig. 3, panel a). Conversely, the large concentration of IPO negative tracks westward (panel c) aligns with the reported findings of Grant and Walsh (2001). Temporal variability showed that TC tracks during the positive (negative) phase are significantly enhanced (suppressed) in terms of length and average speed yet have a shorter (extended) lifetime (Fig. 3, panels d-f). Interestingly, these temporal variations (track length, speed and duration) are also evident for TCs influenced by IOD E positive and negative phases (Fig. 4, panels d-f). Further, the temporal characteristics of the TC tracks are shown to be opposite with respect to EN and LN conditions, possibly due to differences in the TC seasonal cycle of the Indian Ocean and SWP region (Saji et al. 1999; Magee and Verdon-Kidd 2018).

Unlike the typical eastward and westward modulation of TC tracks observed for Pacific and Indian Ocean modes, positive and negative SAM produced northward and southward shifts in SWP TC activity, respectively (Fig. 5, panels a-c). These variations are attributable to the dynamics of SAM, i.e. lower pressure (over Antarctica) with strengthened westerly winds (around Antarctica) and higher pressure in the mid-latitudes, causing alteration of storm tracks more towards the South Pole during positive SAM (opposite for negative SAM) (Renwick and Thompson 2006; Ho et al. 2012; Diamond and Renwick 2015). It was also revealed that SAM positive/negative conditions resulted in westward/eastward modulation of TC tracks. On a broader scale, variations due to SAM are associated with extratropical cyclones or mid-latitude cyclones. Spatial variation in TC tracks during SAM positive indicates that most southern island nations of SWP are at elevated risk, e.g. New Zealand. However, our findings demonstrate that the risk impact for New Zealand (along with other island nations) is amplified during negative SAM.

4.2 Variability in TC tracks by combined climate drivers

Evaluation of climate drivers (i.e. IOD E, IPO and SAM) in combination with the canonical ENSO phases highlighted notable variations in the typical spatio-temporal variability of SWP TCs. Compared with the established eastern and western modulation by the EN and LN phases (Chand and Walsh 2009; Camargo et al. 2010; Chand et al. 2013), it was shown that with some climate mode/index pairings, these modulations could be enhanced or reversed. For instance, EN/IPO negative influenced TC

tracks resulted in westward modulation, demonstrating IPO negative's dominant influence over TC tracks during EN. Magee et al. (2017) reported a similar regime for IPO negative over EN and attributed this variation to the dynamic conditions of this pairing (i.e. conducive relative vorticity and vertical wind shear). In this paper, we also find that these phase pairings substantially suppressed track length and average speed, while a negligible difference was observed for TC duration (enhanced by 1%). The leading influence of IPO negative is also exhibited when paired with LN, where TC duration is enhanced while other temporal attributes are suppressed. A possible reason for such variation could be attributed to the characteristics of western SWP TC tracks, i.e. generally intricate, as reported by Sharma et al. (2021).

The results also demonstrated that both positive and negative phases of IOD E produce notable variations on ENSO influenced TC tracks. Magee and Verdon-Kidd (2018) reported that couplings such as EN/IOD E positive and LN/IOD E negative result in significant spatial modulation of TC genesis. Our findings show that these combinations also influence TC tracks, i.e. EN/IOD E positive (LN/IOD E negative) enhances TC track length and average speed (TC track length and duration) by 13% and 10% (4% and 11%), respectively. The modulation observed during these pairings, i.e. EN/IOD E positive and LN/IOD E negative, are mainly evident on TC tracks within the eastern and western SWP region, respectively, complementing the findings of Sharma et al. (2021). Furthermore, it was shown that ENSO neutral/IOD E negative pairing significantly resulted in the suppression (enhancement) of track length and average speed (duration) by 21% and 16% (6%), respectively. Importantly, this pairing highlights that modulations in SWP TC tracks can occur regardless of ENSO (i.e. during ENSO neutral conditions) through variations in the Indian Ocean SSTs.

A particularly interesting pairing was ENSO and SAM, which provided greater insight into these variations than that provided when these modes were assessed individually. In particular, the lengthening/shortening of TC tracks during LN/EN conditions was shown to be significantly influenced by the positive/negative phases of SAM, respectively, across distinct regions of the SWP. For example, the interaction between EN/SAM negative (both modulating TC activity eastward) resulted in shorter tracks over the eastern part of the SWP, while usually, the tracks are lengthier within this region based on the findings of Sharma et al. (2021). The co-influence of these two modes of climate variabilities (ENSO and SAM) on TC tracks is vital to the broader SWP region and the island nations within the extratropical region (beyond 25°S latitude)—e.g. New Zealand and the southeast coast of Australia. These findings may be used to quantify TC-related hazards better, considering both ENSO and SAM in future TC-related climate attribution studies. For instance, Adam et al. (2021) has shown potential impacts of ENSO and SAM in influencing TCs (later as extratropical cyclones) that results in storm surges. With this information, preparedness and mitigation plans can be enhanced. Furthermore, the westward variation with longer tracks during ENSO neutral and LN conditions (Fig. 2) is generally co-influenced by SAM positive. Complimentary to the findings of Sharma et al. (2021), the effects on the nature of TC tracks (e.g. fast-moving, more prolonged and transitioning into extratropical cyclones) within the western SWP are potentially a result of this co-influential relationship. Indeed, recent events such as TC Gabrielle (2023) that had devastating impact over New Zealand could be attributed to this co-influential relationship, given this event occurred when the state of ENSO was LN (although weakening) and SAM was in positive phase (Australian Bureau of Meteorology 2023; Harrington et al. 2023).

4.3 TC risk impact induced by Pacific and remote climate drivers

TC risk impact analyses have provided insights into how this risk varies for SWP island nations, atolls and territories during various phases of Pacific and remote climate drivers. In many cases, the results demonstrated that TC-induced impacts for island nations are amplified because of each climate phase's spatio-temporal modulation. For example, eastern (western) SWP island nations are more at risk during positive (negative) phases of ENSO, IPO and IOD E. However, in some cases, central SWP island nations are equally impacted during both positive and negative phases—e.g. Fiji during EN and LN. Some interesting cases were revealed where island nations were found to be at risk regardless of their geographical location or the typical spatial modulation exhibited by climate drivers. These occurrences were countered through risk impact assessment of the multimodal analysis. For instance, the impact of EN influenced TCs on western island nations was influenced by the negative phase of IPO. This again highlights the importance of considering multimodal analysis influencing TC track variability. It was also found that irrespective of each climate driver's positive and negative phases, island nations are also vulnerable during the neutral phase.

5 Conclusions

While ENSO is known as the dominant mode of variability within the SWP region, we show that it is not the only factor influencing TC track behaviour. Indeed, IPO, IOD E and SAM also play important roles in the overall prevailing track trajectories. Further, the findings of this study demonstrated that these modes of climate variability do not operate in isolation due to the dynamic nature of the ocean–atmosphere system and hence, modulate the impact of individual drivers. Indeed, the multimodal approach revealed important and distinct trends that were not reflected when climate modes were evaluated individually. It follows that when two climate modes/indices were in phase (e.g. EN with the positive phase of IPO, IOD E and SAM), TC track length and average speed were enhanced. For cases where either one (e.g. EN/negative phase of IPO and IOD E) or both (LN/negative phase of IPO, IOD E and SAM) climate modes/indices were in the negative phase, an increase in TC track duration was observed, implying a dominant impact of negative phases. We also show how variability in TC tracks induced by Indo-Pacific climate drivers imposes a risk impact on SWP island nations. The outcomes of this study, along with statistical or numerical modelling, could be useful in refining forecasts of TC paths once they form and may assist in improved quantification of TC-related risks.

Acknowledgements Krishneel K. Sharma would like to acknowledge the financial contribution from the University of Newcastle (UoN), which provided an International Postgraduate Research Scholarship (UNIPRS) and Research Scholarship Central (UNRSC50:50) for funding his Research Higher Degree (RHD) program at UoN. The authors would also like to thank Olivier Rey-Lescure at the UoN for technical assistance with spatial analysis and mapping. Also, thanks to Cathy Smith, Senior Associate Scientist at NOAA/ESRL Physical Sciences Division (Boulder, Colorado), for valuable insights on re-analysis data (ERSSTv5 and NCEP-NCAR) that was accessed from their website (https://www.esrl.noaa.gov/psd/data/gridded/). The authors declare that there are no conflicts of interest regarding the publication of this article.

Author contributions KKS contributed to data curation, formal analysis, investigation, validation, software, visualization, writing—original draft, project administration, conceptualization and methodology. DVK

contributed to conceptualization, methodology, supervision and writing—review and editing. ADM contributed to conceptualization, methodology, supervision and writing—review and editing.

Funding Open Access funding enabled and organised by CAUL and its Member Institutions. This study was funded by the University of Newcastle (UoN) through their International Postgraduate Research Scholarship (UNIPRS) and Research Scholarship Central (UNRSC50:50), that was awarded to Krishneel K. Sharma for Research Higher Degree (RHD) program.

Declarations

Conflict of interests The authors have no relevant financial or non-financial interests to disclose.

References

Adam RJ, Hilton MJ, Jowett T, Stephenson WJ (2021) The magnitude and frequency of storm surge in southern New Zealand. New Zeal J Mar Freshw Res 55:336–351. https://doi.org/10.1080/00288330.2020.1764596

Andrew NL, Bright P, de la Rua L, Teoh SJ, Vickers M (2019) Coastal proximity of populations in 22 Pacific Island Countries and Territories. PLoS ONE 14(9):e0223249. https://doi.org/10.1371/journal.pone.0223249

Ashok K, Saji NH (2007) On the impacts of ENSO and Indian Ocean dipole events on sub-regional Indian summer monsoon rainfall. Nat Hazards 42(2):273285. https://doi.org/10.1007/s11069-006-9091-0

Australian Bureau of Meteorology (2018) Climate Driver Update archive: Climate drivers in the Pacific, Indian and Southern oceans and the Tropics. http://www.bom.gov.au/climate/enso/wrap-up/archive/20180213.archive.shtml. Accessed 22 Jun 2023

Australian Bureau of Meteorology. (2020). Climatology of Tropical Cyclones in Western Australia. Available at: http://www.bom.gov.au/cyclone/climatology/wa.shtml (Accessed: 31 October 2020).

Australian Bureau of Meteorology (2023) Climate Driver Update archive: Climate drivers in the Pacific, Indian and Southern oceans and the Tropics. http://www.bom.gov.au/climate/enso/wrap-up/archive/20230117.archive.shtml. Accessed 22 Jun 2023

Camargo SJ, Sobel AH, Barnston AG, Klotzbach PJ. (2010) The influence of natural climate variability on tropical cyclones, and seasonal forecasts of tropical cyclone activity. In *Global perspectives on tropical cyclones: From science to mitigation* (pp. 325–360). https://doi.org/10.1142/9789814293488_0011

Chand SS, Walsh KJE (2009) Tropical cyclone activity in the Fiji region: spatial patterns and relationship to large-scale circulation. J Clim 22(14):3877–3893. https://doi.org/10.1175/2009JCLI2880.1

Chand SS, McBride JL, Tory KJ, Wheeler MC, Walsh KJE (2013) Impact of different ENSO regimes on Southwest Pacific tropical cyclones. J Clim 26(2):600–608. https://doi.org/10.1175/jcli-d-12-00114.1

Chand SS, Chand SS, Tory KJ, Dowdy AJ, Turville C, Ye H (2019) Projections of southern hemisphere tropical cyclone track density using CMIP5 models. Clim Dyn 52(910):60656079. https://doi.org/10.1007/s00382-018-4497-4

Christensen JH, Kanikicharla KK, Aldrian E, An S-I, Cavalcanti IFA, de Castro M, Dong W, Goswami P, Hall A, Kanyanga JK, Kitoh A, Kossin J, Lau N-C, Renwick J, Stephenson DB, Xie S-P, Zhou T, Press CU (2013) Climate phenomena and their relevance for future regional climate change. In: Stocker TF, Qin D, Planttner G-K, Tignor M, Allen SK, Boschung J, Nauels A, Zia Y, Bex V, Midgley PM (eds) Climate change the physical science basis. contribution of working Group I to the Fifth Assessment report of the intergovernmental panel on climate change. Cambridge University Press, Cambridge, USA

Diamond HJ, Renwick JA (2015) The climatological relationship between tropical cyclones in the southwest pacific and the southern annular mode. Int J Climatol 35(4):613–623. https://doi.org/10.1002/joc.4007
Diamond HJ, Lorrey AM, Knapp KR, Levinson DH (2012) Development of an enhanced tropical cyclone tracks database for the southwest Pacific from 1840 to 2010. Int J Climatol 32(14):2240–2250. https://doi.org/10.1002/joc.2412
Diamond HJ, Lorrey AM, Renwick JA (2013) A Southwest Pacific tropical cyclone climatology and linkages to the El NiñoSouthern oscillation. J Clim 26(1):325. https://doi.org/10.1175/JCLI-D-12-00077.1
EM-DAT. (2020). The International Disaster Database, Centre for Research on Epidemiology of Disasters - CRED. Available at: https://public.emdat.be/data (Accessed: 11 August 2020).
Flanders Marine Institute. (2018). Maritime Boundaries Geodatabase: Maritime Boundaries and Exclusive Economic Zones (200NM), Version 10. Available at: https://www.marineregions.org/ (Accessed: 23 November 2021).
Gong D, Wang S (1999) Definition of antarctic oscillation index. Geophys Res Lett 26(4):459–462. https://doi.org/10.1029/1999GL900003
Grant AP, Walsh KJE (2001) Interdecadal variability in north-east Australian tropical cyclone formation. Atmosph Sci Lett 2(1):9–17. https://doi.org/10.1006/asle.2001.0029
Harrington LJ, Dean SM, Awatere S, et al (2023) The role of climate change in extreme rainfall associated with Cyclone Gabrielle over Aotearoa New Zealand's East Coast. https://doi.org/10.25561/102624
Henley BJ, Gergis J, Karoly DJ, Power S, Kennedy J, Folland CK (2015) A tripole index for the interdecadal Pacific oscillation. Clim Dyn 45(11–12):3077–3090
Ho M, Kiem AS, Verdon-Kidd DC (2012) The Southern Annular Mode: a comparison of indices. Hydrol Earth Syst Sci 16(3):967–982. https://doi.org/10.5194/hess-16-967-2012
Holland GJ (1981) On the quality of the Australian tropical cyclone data base. Aust Met Mag 29:169181
Holland GJ, Lander M (1993) The meandering nature of tropical cyclone tracks. J Atmos Sci 50(9):12541266. https://doi.org/10.1175/1520-0469(1993)050%3c1254:TMNOTC%3e2.0.CO;2
Holland, G. J., & Gray, W. M. (1983). Tropical cyclones in the Australian/southwest Pacific region. *Atmospheric Science Paper; No. 363*.
Huang B, Thorne PW, Banzon VF, Boyer T, Chepurin G, Lawrimore JH, Menne MJ, Smith TM, Vose RS, Zhang H-M (2017a) Extended reconstructed sea surface temperature, Version 5 (ERSSTv5): upgrades, validations, and intercomparisons. J Clim 30(20):8179–8205. https://doi.org/10.1175/jcli-d-16-0836.1
Huang B, Thorne PW, Banzon VF, Boyer T, Chepurin G, Lawrimore JH, Menne MJ, Smith TM, Vose RS, Zhang H-M (2017b) NOAA extended reconstructed sea surface temperature (ERSST), Version 5. NOAA Nat Centers Environ Inform. https://doi.org/10.7289/V5T72FNM
Kidson JW, Sinclair MR (1995) The influence of persistent anomalies on southern hemisphere storm tracks. J Clim 8(8):19381950. https://doi.org/10.1175/1520-0442(1995)008%3c1938:Tiopao%3e2.0.Co;2
Kidston J, Gerber EP (2010) Intermodel variability of the poleward shift of the austral jet stream in the CMIP3 integrations linked to biases in 20th century climatology. Geophys Res Lett. https://doi.org/10.1029/2010GL042873
Kossin JP, Emanuel KA, Vecchi GA (2014) The poleward migration of the location of tropical cyclone maximum intensity. Nature 509:349352. https://doi.org/10.1038/nature13278
Kousky VE, Higgins RW (2007) An alert classification system for monitoring and assessing the ENSO Cycle. Weather Forecast 22(2):353–371. https://doi.org/10.1175/waf987.1
Liu KS, Chan JCL (2012) Interannual variation of Southern Hemisphere tropical cyclone activity and seasonal forecast of tropical cyclone number in the Australian region. Int J Climatol 32(2):190–202
Magee AD, Verdon-Kidd DC (2018) On the relationship between Indian Ocean sea surface temperature variability and tropical cyclogenesis in the southwest Pacific. Int J Climatol 38:e774–e795. https://doi.org/10.1002/joc.5406
Magee AD, Verdon-Kidd DC, Kiem AS (2016) An intercomparison of tropical cyclone best-track products for the southwest Pacific. Nat Hazard 16(6):1431–1447. https://doi.org/10.5194/nhess-16-1431-2016
Magee AD, Verdon-Kidd DC, Diamond HJ, Kiem AS (2017) Influence of ENSO, ENSO Modoki, and the IPO on tropical cyclogenesis: a spatial analysis of the southwest Pacific region. Int J Climatol 37:1118–1137. https://doi.org/10.1002/joc.5070
Magee AD, Lorrey AM, Kiem AS, Colyvas K (2020) A new island-scale tropical cyclone outlook for southwest Pacific nations and territories. Sci Rep 10(1):1–13. https://doi.org/10.1038/s41598-020-67646-7
Malsale P (2011) Analysis of Tropical Cyclone Track Sinuosity in the South Pacific Region using ArcGIS. The University of the South Pacific, Fiji
Marshall GJ (2003) Trends in the Southern Annular Mode from Observations and Reanalyses. J Clim 16(24):4134–4143. https://doi.org/10.1175/1520-0442(2003)016%3c4134:Titsam%3e2.0.Co;2
Murakami H, Delworth TL, Cooke WF, Zhao M, Xiang B, Hsu PC (2020) Detected climatic change in global distribution of tropical cyclones. Proc Natl Acad Sci USA 117(20):1070610714. https://doi.org/10.1073/pnas.1922500117

Naylor AK (2015) Island morphology, reef resources, and development paths in the Maldives. Prog Phys Geogr 39(6):728–749. https://doi.org/10.1177/0309133315598269
Neumann B, Vafeidis AT, Zimmermann J, Nicholls RJ (2015) Future coastal population growth and exposure to sea-level rise and coastal flooding—a global assessment. PLoS ONE 10(3):e0118571. https://doi.org/10.1371/journal.pone.0118571
Ramsay HA, Camargo SJ, Kim D (2012) Cluster analysis of tropical cyclone tracks in the Southern Hemisphere. Clim Dyn 39(3):897–917. https://doi.org/10.1007/s00382-011-1225-8
Ramsay HA, Richman MB, Leslie LM (2017) The modulating influence of indian ocean sea surface temperatures on australian region seasonal tropical cyclone counts. J Clim 30(13):48434856. https://doi.org/10.1175/jcli-d-16-0631.1
Renwick J, Thompson D (2006) The southern annular mode and New Zealand climate. Water Atmos 14(2):24–25
Saha KK, Wasimi SA (2013) Interrelationship between Indian Ocean Dipole (IOD) and Australian tropical cyclones. Int J Environ Sci Develop 4(6):647651. https://doi.org/10.7763/IJESD.2013.V4.431
Saji NH, Goswami BN, Vinayachandran PN, Yamagata T (1999) A dipole mode in the tropical Indian Ocean. Nature 401(6751):360–363. https://doi.org/10.1038/43854
Saverimuttu V, Varua ME (2017) Managing the socioeconomic impacts of extreme weather events in the southwest pacific basin. Int J Safety Secur Eng 7(2):201–212. https://doi.org/10.2495/SAFE-V7-N2-201-212
Sharma KK, Verdon-Kidd DC, Magee AD (2020) Decadal variability of tropical cyclogenesis and decay in the southwest Pacific. Int J Climatol 40(5):2811–2829. https://doi.org/10.1002/joc.6368
Sharma KK, Magee AD, Verdon-Kidd DC (2021) Variability of southwest Pacific tropical cyclone track geometry over the last 70 years. Int J Climatol 41(1):529–546. https://doi.org/10.1002/joc.6636
Sharmila S, Walsh KJE (2018) Recent poleward shift of tropical cyclone formation linked to Hadley cell expansion. Nat Clim Chang 8(8):730736. https://doi.org/10.1038/s41558-018-0227-5
Sinclair MR (2002) Extratropical transition of southwest pacific tropical cyclones. Part I Climatology and mean structure changes. Monthly Weather Rev 130(3):590–609
Small C, Nicholls RJ (2003) A global analysis of human settlement in coastal zones. Source J Coast Res 19(3):584–599
Stephens SA, Ramsay DL (2014) Extreme cyclone wave climate in the Southwest Pacific ocean: influence of the el niño southern oscillation and projected climate change. Global Planet Change 123:1326. https://doi.org/10.1016/j.gloplacha.2014.10.002
Terry JP (2007) Tropical cyclones: climatology and impacts in the South Pacific. Springer Science & Business Media Springer, New York
World Meteorological Organization. (2017). WMO Guidelines on the Calculation of Climate Normals (WMO/TD-No. 1203), Geneva, Switzerland: World Meteorological Organisation.
Yin JH (2005) A consistent poleward shift of the storm tracks in simulations of 21st century climate. Geophys Res Lett. https://doi.org/10.1029/2005GL023684